Macromolecular Research, Vol. 16, No. 2, pp 139-148 (2008)

Preparation and Characterization of Temperature-Sensitive Poly(*N*-isopropylacrylamide)-*g*-Poly(L-lactide-*co*-ε-caprolactone) Nanofibers

Sung In Jeong and Young Moo Lee

School of Chemical Engineering, College of Engineering, Hanyang University, Seoul 133-791, Korea

Joohyeon Lee, Young Min Shin, and Heungsoo Shin*

Department of Bioengineering, College of Engineering, Hanyang University, Seoul 133-791, Korea

Youn Mook Lim and Young Chang Nho

Radiation Application Research Division, Advanced Radiation Technology Institute, Korea Atomic Energy Research Institute, Jeonbuk 580-195, Korea

Received August 29, 2007; Revised October 29, 2007

Abstract: Biodegradable and elastic poly(L-lactide-*co*-ε-caprolactone) (PLCL) was electrospun to prepare nanofibers, and *N*-isopropylacrylamide (NIPAAm) was then grafted onto their surfaces under aqueous conditions using ^{60}Co-γ irradiation. The graft yield increased with increasing irradiation dose from 5 to 10 kGy and the nanofibers showed a greater graft yield compared with the films. SEM confirmed that the PLCL nanofibers maintained an interconnected pore structure after grafting with NIPAAm. However, overdoses of irradiation led to the excessive formation of homopolymer gels on the surface of the PLCL nanofibers. The equilibrium swelling and deswelling ratio of the PNIPAAm-*g*-PLCL nanofibers (prepared with 10 kGy) was the highest among the samples, which was consistent with the graft yield results. The phase-separation characteristics of PNIPAAm in aqueous conditions conferred a unique temperature-responsive swelling behavior of PNIPAAm-*g*-PLCL nanofibers, showing the ability to absorb a large amount of water at < 32 °C, and abrupt collapse when the temperature was increased to 40 °C. In accordance with the temperature-dependent changes in swelling behavior, the release rate of indomethacin and FITC-BSA loaded in PNIPAAm-*g*-PLCL nanofibers by a diffusion-mediated process was regulated by the change in temperature. Both model drugs demonstrated greater release rate at 40 °C relative to that at 25 °C. This approach of the temperature-controlled release of drugs from PNIPAAm-*g*-PLCL nanofibers using gamma-ray irradiation may be used to design drugs and protein delivery carriers in various biomedical applications.

Keywords: electrospinning, temperature-sensitive, tissue engineering, gamma ray irradiation.

Introduction

Electrospinning is a useful technique for producing nonwoven and highly porous nanofibers with diameters in the nm-μm range.[1,2] Recently, this technology has been used to control the morphology, porosity, and composition of biomaterials for many biomedical applications.[3,4] In particular, the potential of applying micro/nano-scaled scaffolds in tissue engineering is enormous, because the nano-scale dimensions provide a well-defined architecture with high surface area to volume ratio, allowing a favorable microenvironment for tissue growth.[5-10] Thus, tissue engineering with scaffolds has been focused on the production of an ideal three-dimensional nanofibrous structure capable of reconstituting natural extracellular matrix (ECM) and allowing for the subsequent proliferation of seeded cells, thereby stimulating new tissue formation.[11]

To enhance tissue repair and regeneration, growth factors are often loaded within the scaffolds and delivered in a local tissue defect. Although many carriers loaded with growth factors have been proposed for particular types of tissue, the control over the growth factor release from the scaffolds remains a challenge.[12-16] Because tissue regeneration is a highly coordinated process involving many types of growth factors, it is imperative to produce an ideal delivery carrier with the capability of releasing growth factors in a controlled manner. One approach to this problem is the use of a stimuli-sensitive delivery system, which is able to regulate

*Corresponding Author. E-mail: hshin@hanyang.ac.kr

growth factor release in response to external stimuli—such as small changes in pH or temperature—through the change of its swelling behavior, permeability, or mechanical strength.[17,18]

Poly(*N*-isopropylacrylamide)(PNIPAAm) has been used to produce temperature-sensitive drug delivery carriers due to its lower critical solution temperature (LCST) in aqueous conditions at around 32 °C.[3,19-24] PNIPAAm hydrogels exhibit remarkable hydration/dehydration in response to temperature change. Although NIPAAm has been widely employed to prepare hydrogels and films, there has been little study of temperature-responsive nanofibers. Furthermore, grafting NIPAAm to nanofibrous synthetic biodegradable polymers such as poly(L-lactide), poly(glycolide), poly(caprolactone), and their copolymers is more challenging, due to the presence of limited number of functional groups for conjugation with NIPAAm.

In the present study, gamma-ray irradiation was applied to prepare temperature-responsive PNIPAAm-grafted poly(L-lactide-*co*-ε-caprolactone) (PLCL) nanofibers. Gamma-ray irradiation grafting technology is known to be a convenient tool for the surface modification of the morphological and chemical properties of various substrates.[25-28] It is relatively simple to use, and moreover, the ability to modify the internal surface of a 3D matrix can be controlled easily by varying the irradiation dose.[29-32] PLCL has several unique properties such as high elasticity and biocompatibility, and is widely used in scaffolds and drug delivery matrices.[33-35]

Firstly, the effect of irradiation doses on the graft yield of PLCL substrate was investigated. We examined the gamma-ray irradiation technique for introduction of PNIPAAm, comparing the efficacy of addition to PLCL nanofibers and films. Secondly, we examined the graft efficiency on the swelling/deswelling ratio of PNIPAAm-*g*-PLCL substrates in response to temperature change, under both static and pulsatile conditions. Finally, the hydrophobic and hydrophilic model drugs (indomethacin and FITC-BSA, respectively) were loaded in PNIPAAm-*g*-PLCL substrates and their temperature-dependent release behaviors were monitored and compared.

Experimental

Materials. L-Lactide was purchased from Purac Biochem (Netherlands), purified by recrystallization using dried ethyl acetate, and thoroughly dried for 24 h under vacuum prior to use. Stannous octoate, ε-caprolactone, 2,2,2-trifluoroethanol (TFE), NIPAAm, and chloroform were purchased from Sigma Chemical Co. (St. Louis, MO, USA). Toluene and ε-caprolactone were distilled using calcium hydride, and stannous octoate was purified at 175 °C by vacuum distillation (ca. 0.2 mmHg). Dulbecco's phosphate buffered saline (PBS) was purchased from Gibco BRL (Rockville, MD, USA), and water was distilled and deionized using the Milli-Q System (Waters, Millipore, MA, USA). All other chemicals and solvents were of analytical grade and were used without further purification.

Synthesis of PLCL and Preparation of PLCL Nanofibers and Films. PLCL was synthesized as previously described.[36,37] Briefly, equal molar amounts of L-lactide and ε-caprolactone (100 mmol) were co-polymerized, using stannous octoate (1 mmol) as a catalyst, at 150 °C for 24 h in a 50 mL glass ampoule under anhydrous conditions. After the reaction, the product was dissolved in chloroform and micro-filtered, and the purified solution was reprecipitated with an excess amount of methanol. The molar ratio of lactide to caprolactone in the final product was 5.1/4.9 as determined by nuclear magnetic resonance spectroscopy. Gel permeation chromatography confirmed that the number average (M_n) and weight average (M_w) molecular weights were 271,000 and 348,000, respectively.

In order to fabricate nanofibers, PLCL was dissolved in TFE (10% w/v) and directly electrospun to an aluminum foil sheet placed on the collector. Specifically, the PLCL solution was loaded in a 20 mL glass syringe (Hamilton, NV, USA) equipped with a blunt 23 gauge needle. The glass syringe was then placed in a syringe pump (KD Scientific Single-Syringe Infusion Pump, Fisher, MA, USA) and the needle was connected to the positive output of a high voltage power supply (NanoNC, Seoul, Korea). The polymer solution was then electrospun directly to the aluminum foil wrapping around the ground collector (9 cm in diameter), located at a fixed distance of 20 cm from the needle, at room temperature (RT). The flow rate of the solution, applied voltage, and spinning time were set to 2 mL/h, 18-20 kV, and 24 h, respectively. Following the spinning process, the nanofibers were rinsed three times with distilled, deionized water (DDW) to remove any residual chemicals, and dried at RT overnight.

PLCL films were prepared using a solvent casting process. PLCL solution was dissolved in chloroform (20% w/v) for 4 h at RT; 10 mL of the solution was poured into a 70 mm glass dish and dried at 60 °C.

Surface Grafting of NIPAAm Onto PLCL-Based Substrates Using Gamma-Ray Irradiation. NIPAAm was grafted to the surface of the PLCL films and nanofibers using gamma-ray irradiation (Figure 1). The PLCL films and nanofibers were immersed into the NIPAAm solution (1 wt% in water), and exposed to ^{60}Co γ-rays (ACEL type C-1882, Korea Atomic Energy Institute, 2.15×10^5 rad/h, 5 or 10 kGy) at room temperature for 10 h. Following the graft reaction, the samples were washed with DDW three times and soaked in DDW for 72 h in order to remove any residual unreacted NIPAAm monomers, as well as homopolymers that may have been produced during the irradiation process. After thorough rinsing, the samples were dried under vacuum at 50 °C before any measurements. The designation of each sample prepared from different irradiation doses is presented in Table I.

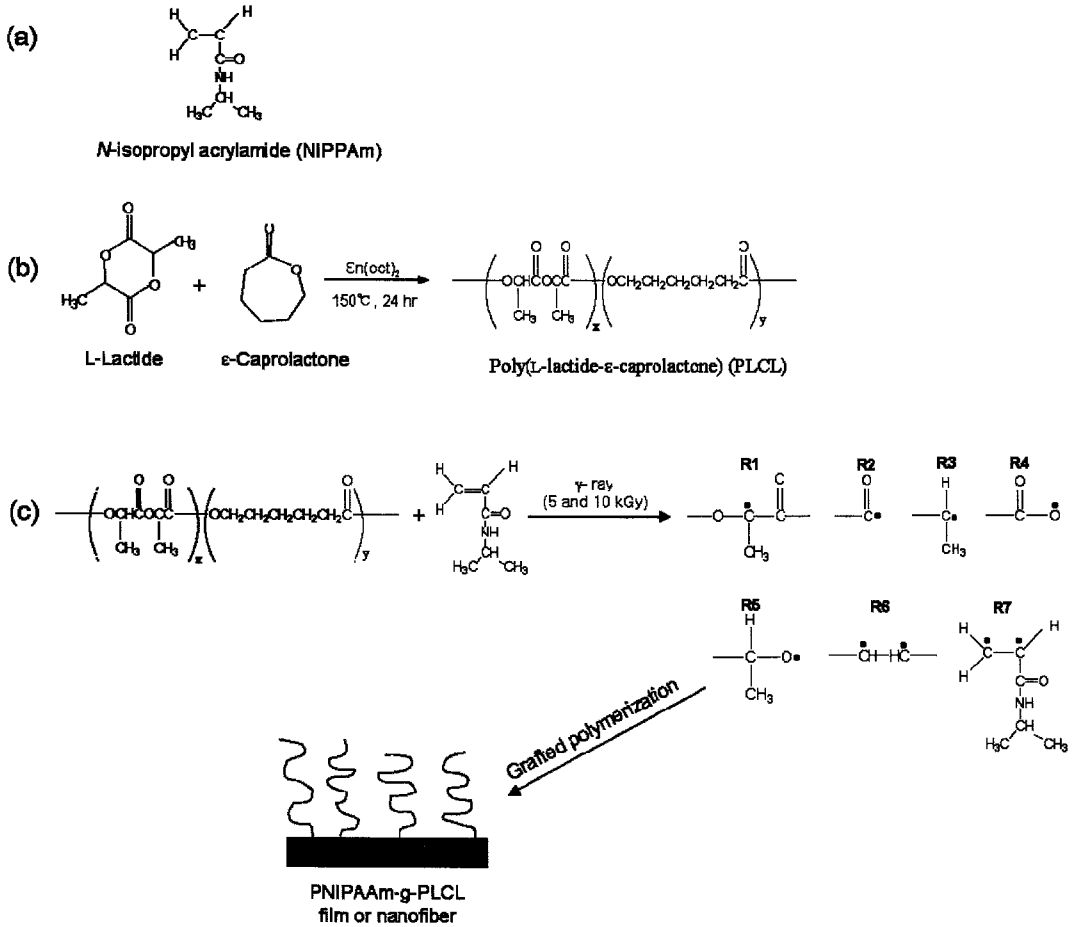

Figure 1. Chemical structures of (a) NIPAAm monomer and (b) PLCL. (c) Schematic illustration of the grafting of NIPAAm onto the surface of PLCL substrates to prepare PNIPAAm-*g*-PLCL films and nanofibers. R1-R7 represent possible structures of radicals formed by gamma-ray irradiation.

Table I. Designation and Preparation Conditions of PNIPAAm-*g*-PLCL Films and Nanofibers Using Various Irradiation Doses

Sample Types	NIPAAm Concentration[a] (wt%)	Irradiation Dose (kGy)
PLCL Film	1	5
	1	10
PLCL Nanofiber	1	5
	1	10

[a]Solvent: water.

Characterizations of the PNIPAAm-*g*-PLCL Films and Nanofibers. The graft yield was measured based on the weight change during irradiation. The samples were weighed before (W_1) and after (W_2) the reaction, and the graft yield was calculated by the following equation of $(W_2-W_1)/W_1(\%)$. The morphology of PNIPAAm-*g*-PLCL substrates was examined using scanning electron microscopy (SEM, JEOL JSM-6300, Japan). The specimens (5 × 5 mm) were obtained before and after the irradiation and they were mounted onto sample studs and coated with gold using a sputter coater (Eiko IB3, Tokyo, Japan) for 5 min. The microscope was operated at 15 kV to visualize the morphology of the samples.

To confirm the presence of functional groups on the surface of the PLCL substrates, attenuated total reflectance fourier transform infrared (ATR-FTIR) spectroscopic measurement was carried out with a Bruker TENSOR 37 (Bruker, MA, USA) spectrophotometer. ATR spectra were recorded at 16 scans with resolution of 4 cm^{-1} and the recording range was between 2000 and 1000 cm^{-1}. The X-ray photoelectron spectroscope (XPS) measurement was performed using an ESCA LAB 220I (Thermo VG Scientific, MA, USA) spectrometer with a magnesium anode source producing Mg Kα (1253.6 eV photons) X-rays, with pass energy of 20 eV for high-resolution narrow scans and 150 eV for low-resolution wide scans.

Swelling Studies of PNIPAAm-*g*-PLCL Films and Nanofibers. To study swelling kinetics in response to temperature change, PNIPAAm-*g*-PLCL film and nanofiber samples were incubated in DDW at 25 °C. The weight of the swollen samples was measured at various time intervals

up to 30 min, after excess water was removed from the sample surface. The swelling ratio was calculated using the following formula:

$$\text{Swelling ratio (\%)} = (W_s - W_d) / W_d \times 100$$

where W_s and W_d are the weight of the samples in the swollen and dry state, respectively. The deswelling kinetics of PLCL samples in response to temperature change were also characterized, by measuring weight change following a rapid increase in temperature from 25 to 40 °C.

The temperature-responsive equilibrium swelling behavior was examined by measuring the swelling ratio of PLCL samples after saturation in DDW for 1 day at each of four different temperatures (25, 30, 37, and 40 °C).

The pulsatile swelling behavior was observed by measuring the swelling ratio at alternating temperatures of 25 and 40 °C. Briefly, the samples were incubated in 40 °C for 5 min and their swelling ratio was measured; the samples were immediately incubated at 25 °C for 5 min and their swelling ratio was measured again. The same procedure was repeated at least six times.

Thermo-Responsive Release of Indomethacin and FITC-BSA. Indomethacin (IMC, 1-[*p*-chlorobenzoyl]-5-methnoxy-2-methylindole-3-acetic acid) and FITC-BSA (Fluorescein isothiocyanate-conjugated bovine serum albumin) were loaded as model drugs in the PNIPAAm-*g*-PLCL films and nanofibers. PLCL film and nanofiber samples grafted with NIPAAm under the irradiation dose of 10 kGy were loaded with each drug via swelling-mediated diffusion. Known solutions of IMC (20% w/v) in ethyl alcohol and FITC-BSA (10% w/v) in PBS (pH 7.4) were prepared, and the samples (size = 1 × 1 cm) were soaked in the drug solutions for 2 days at 25 °C. The samples were then blotted with filter paper to eliminate the surface water and dried at room temperature for 1 day.

The pulsatile drug release kinetics were observed by measuring the cumulative amount of the drug released at temperatures alternating between 25 and 40 °C four times. The samples were incubated in 25 °C for 30 min and the drug release was measured; after this the samples were immediately subjected to incubation at 40 °C for an additional 15 min and their drug release was again measured. The amount of IMC released was analyzed using a HPLC spectrophotometer (YoungLin, Model UV730D, Seoul, Korea). Solutions with known concentrations of IMC were used to obtain the standard curve. The amount of released FITC-BSA was determined with a microplate reader (λ_{ex} 485 nm, λ_{em} 535 nm, Tecan Spectra Fluor Plus, MTX Lab Systems, VA, USA).

Results and Discussion

Grafting of NIPAAm on PLCL Films and Nanofibers. For both electrospun nanofibers and solvent-cast PLCL films, we found that graft yield increased with increasing irradiation doses (Figure 2). When NIPAAm was grafted onto the PLCL film, the graft ratio was increased from 0.05 ± 0.31% at 5 kGy to 0.43 ± 0.13% at 10 kGy. The nanofibers demonstrated the same trend, but with considerably higher graft yield: 0.99 ± 0.11% at 5 kGy and 2.43 ± 0.65% at 10 kGy. Graft yield can be regulated by various irradiation parameters, including the concentration of monomers (NIPAAm in our study), solvent type, reaction temperature, and irradiation dose.[38-40] It has been widely established that the irradiation dose is the predominating factor in controlling the graft yield. Consistent with previous reports from other groups and our laboratories, the amount of grafted NIPAAm onto the substrates appeared to be proportional to the irradiation dose.[38-41]

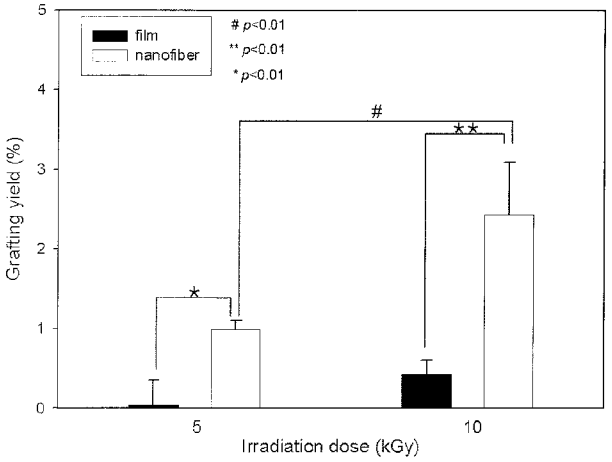

Figure 2. Graft yields of PNIPAAm-*g*-PLCL films and nanofibers prepared with two different irradiation doses.

In an attempt to improve the graft yield, we increased the irradiation dose above 10 kGy. However, this led to the formation of PNIAAm homopolymer gels on the PLCL substrate. The samples were extensively rinsed with DDW, but the homopolymer gels appeared to be permanently attached to the surface of the PLCL substrate. Therefore, 10 kGy may be the maximum irradiation dose tested in our study that minimizes the formation of the homopolymer gels on the surface. Further improvements in the graft yield of PNIPAAm-*g*-PLCL substrates may require the manipulation of other conditions, such as the addition of non-solvent to water (the current solvent) or adjustment of the monomer concentration.

PLCL nanofibers showed significantly higher graft yield than PLCL films. The increased graft yield for nanofibers may be attributed to their greater surface area. Although we did not quantitatively measure the surface area of the nanofibers, the previous study has emphasized the advantages of using nanofibers as drug delivery carriers or tissue engineering scaffolds due to their greater surface area.[42] Particularly, the electrospinning process proved to be an effec-

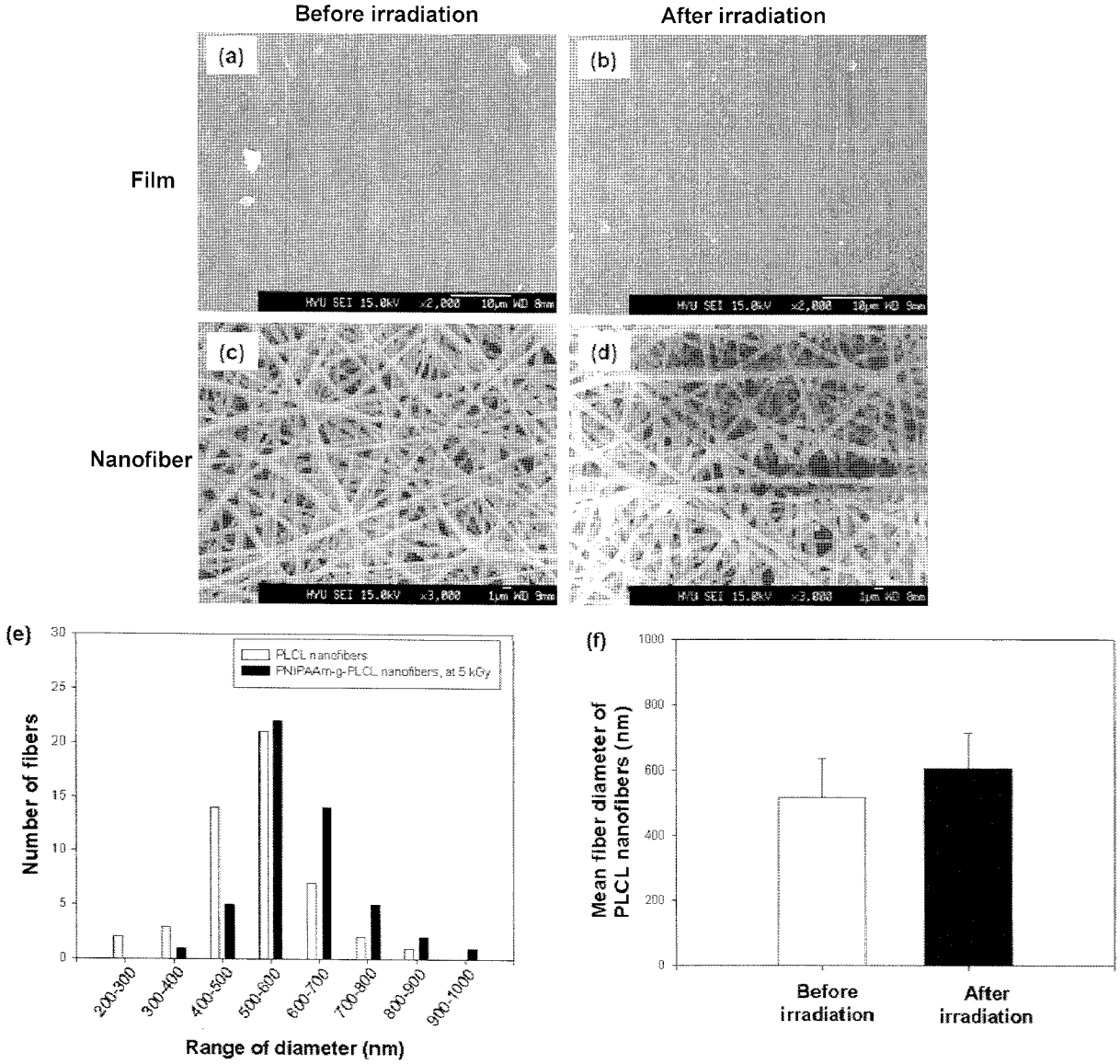

Figure 3. SEM images and mean fiber diameters of PNIPAAm-*g*-PLCL films and nanofibers. PLCL films (a) before and (b) after 5-kGy irradiation dose, respectively, and PLCL nanofibers (c) before and (d) after 5-kGy irradiation dose. The (e) distribution of number of fibers over ranges of fiber diameter where fiber diameters were measured from randomly chosen SEM images and (f) mean fiber diameter of PNIPAAm-*g*-PLCL films and nanofibers prepared under the irradiation of 5 kGy.

tive source for the generation of a nanofibrous structure comprising nano-scaled, non-woven, and interconnected pores with a high surface area to volume ratio. Our results are in good agreement with previous reports, suggesting that nanofibers provide a greater platform for the grafting of biologically functional groups by leading to higher graft yield to the gamma-ray irradiation technique than 2-dimensional films.

Characterizations of the PNIPAAm-*g*-PLCL Films and Nanofibers.[43] Gamma ray irradiation did not alter the surface morphology of the PLCL films (Figure 3). The SEM image of nanofibers before and after 5 kGy irradiation also confirmed minimal change in the fiber diameter. For the quantitative analysis, we chose more than 50 fibers from randomly chosen 5 different fields of images and manually measured their diameters using Photoshop. The largest number of fibers were between 500 and 600 nm in diameter, before and after irradiation (Figure 3(e)). Although the distribution of fiber diameters of nanofibers after irradiation was shifted right-sided as compared to that before irradiation, indicating slight increase in the fiber diameter, the mean diameter was not statistically different. These results suggest that the irradiation doses tested in our study successfully introduced desirable functional groups on the sur-

face of PLCL nanofibers without significant deformation of the three-dimensional interconnected fibrous structure. When we prolonged irradiation time and doses over 10 kGy, surface gelation of PNIPAAm homopolymers was evident. The SEM images (data not shown) demonstrated that these homopolymers often closed open pores between the nanofibers and that the fiber diameters were significantly increased. Although the gelation of PNIPAAm during the surface grafting process has been reported elsewhere,[40] the grafting of PNIPAAm onto the nanofiber matrix, particularly biodegradable elastic PLCL, has not to our knowledge been previously studied. Therefore, the optimization of grafting conditions by changing the solvent or the monomer concentration may be an attractive topic for further investigation (the tensile testing of the nanofiber specimen demonstrated that the tensile strength and Young's modulus were both slightly decreased from 1.8 ± 0.3 to 1.1 ± 0.4 (kgf/mm^2) and 0.41 ± 0.02 to 0.30 ± 0.02 (kgf/mm^2), respectively. However, the elongation at break of the nanofibers were from 159.5 ± 15.2 to 146.2 ± 36.5 following the irradiation process, which was statistically consistent. Despite the reduced tensile strength and Young's modulus, the nanofibers maintained elastic properties and were mechanically stable during the whole experiment).

The surface properties of the PNIPAAm-*g*-PLCL films and nanofibers were characterized by ATR-FTIR and XPS measurements. The characteristic peak for PLCL was detected at 1769 cm^{-1} in all groups, indicating the presence of ester groups,[44] while two additional peaks at 1540 and 1656 cm^{-1} were observed in PNIPAAm-grafted samples (Figure 4(a)). These bands are attributed to secondary amide C=O stretching and N-H stretching of present in NIPAAm polymer chains, suggesting the successful grafting of NIPAAm to the PLCL substrate.[39,45] Notably, the intensity of these two bands in PNIPAAm-*g*-PLCL fibers was greater than those in PNIPAAm-*g*-PLCL films, indicating that the amount of grafted PNIPAAm may be correspondingly greater. Together with the results from quantitative measurement of the graft yield, this suggests that nanofibers produce greater graft yield under the conditions tested.

XPS indicates the presence of nitrogen atoms on the surface of the PNIPAAm-*g*-PLCL films and nanofibers (Figure 4(b)). PLCL showed only C 1s and O 1s peaks presented at binding energies of ca. 291 and 530 eV, respectively, and the peak area ratio of O 1s/C 1s was also found to be in good agreement with the theoretical values of O/C in PLCL (data not shown). In addition, we observed the presence of N 1s peak at 399 eV in PNIPAAm-*g*-PLCL films and nanofibers, which was consistent with previous results.[46,47]

Swelling and Deswelling of PNIPAAm-*g*-PLCL Substrates. All samples demonstrated rapid swelling and reached an equilibrium swelling state within 5 min (Figure 5). The swelling ratios of nanofibers were greater than those of PNIPAAm-*g*-PLCL films fabricated under the same conditions. For example, the equilibrium swelling ratio (after 10 min of swelling) of PNIPAAm-*g*-PLCL films irradiated with 5 kGy was 0.45 ± 0.75%, which was increased to 9.53 ± 3.24% for PNIPAAm-*g*-PLCL nanofibers irradiated with the same dose. The swelling ratio of PNIPAAm-*g*-PLCL nanofibers prepared by irradiation of 10 kGy was the highest (41.16 ± 4.05%) among the samples, which may be due to their high graft yield.[20,48,49] Although the swelling ratio of the samples was consistent with graft yield, it is not clear whether all the grafted PNIPAAm was crosslinked with other chains or maintained single chains to serve as polymer brushes. Gamma-ray irradiation can generate a large number of radicals, which indeed facilitate grafting as well as crosslinking of NIPAAm to PLCL substrates in the reaction solution. However, it is also difficult to control the cleavage sites where new radicals are formed.

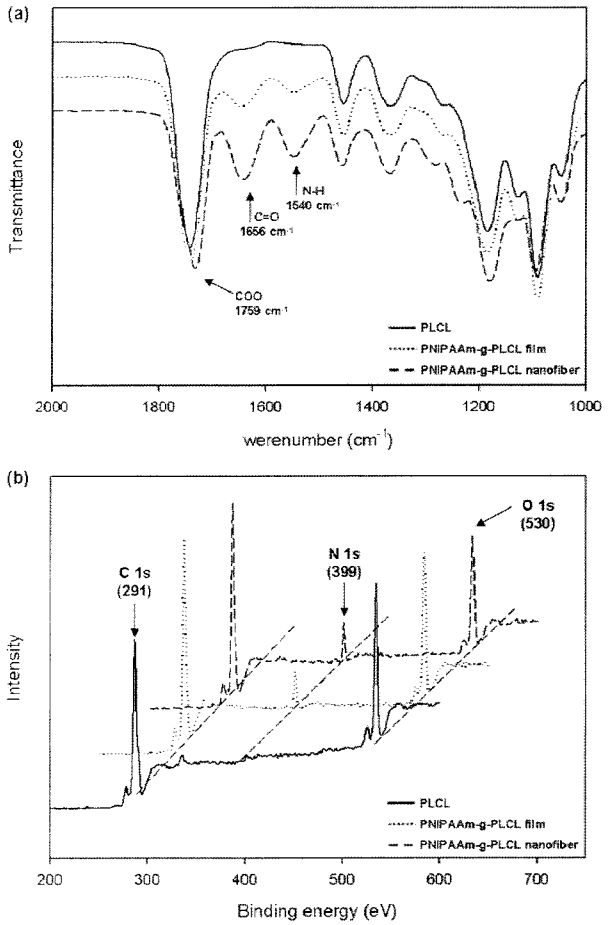

Figure 4. Surface chemical properties of PNIPAAm-*g*-PLCL films and nanofibers. (a) ATR-FTIR and (b) XPS spectra of the samples.

Deswelling occurred within 10 min, with the same trends as observed for the swelling kinetics (Figure 5(b)). The deswelling ratio of PNIPAAm-*g*-PLCL nanofibers prepared with 10 kGy irradiation was 84.27 ± 6.48%, which was the great-

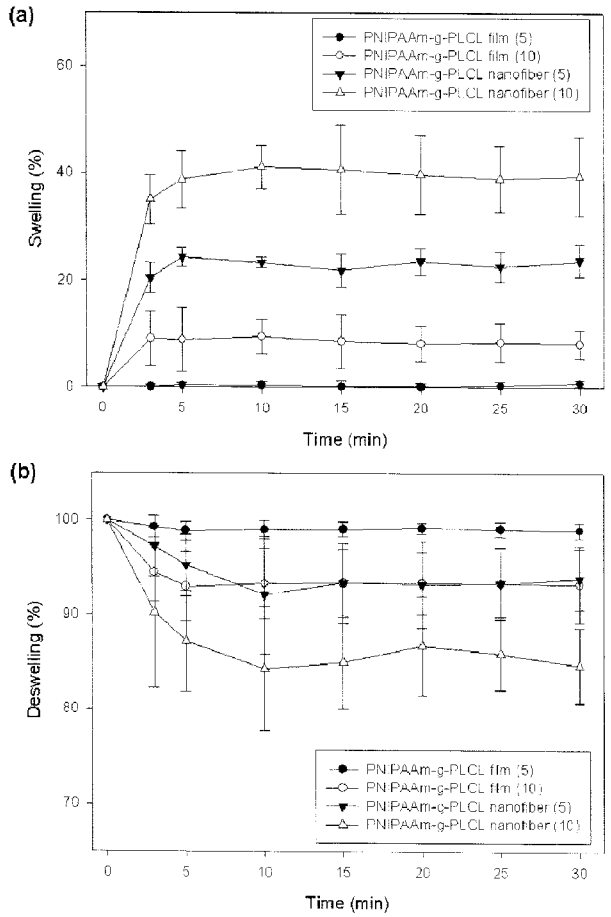

Figure 5. Swelling and deswelling kinetics of PNIPAAm-*g*-PLCL films and nanofibers in deionized water at (a) 25 °C and (b) 40 °C.

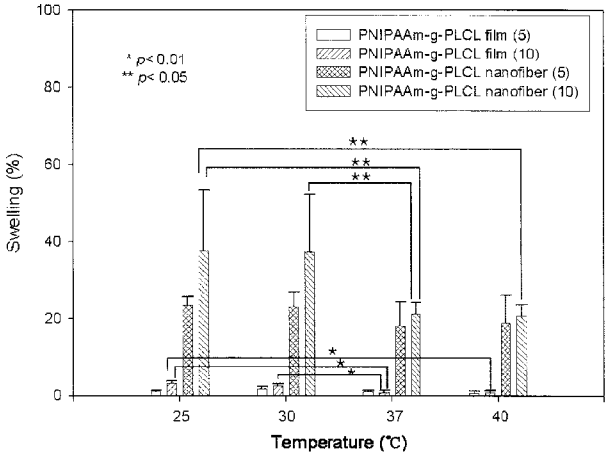

Figure 6. Equilibrium swelling ratios of PNIPAAm-*g*-PLCL films and nanofibers in deionized water in response to temperature change.

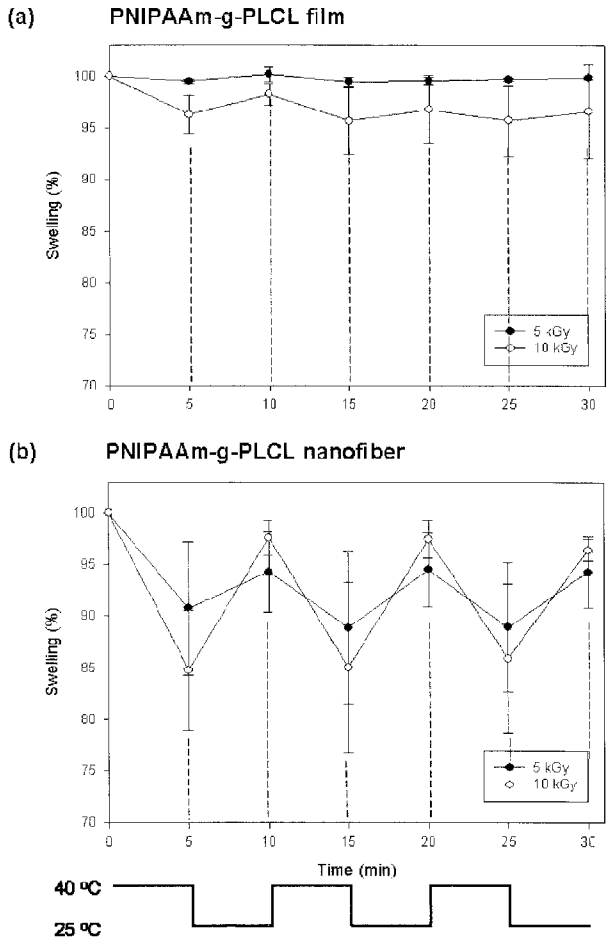

Figure 7. Pulsatile swelling kinetics of PNIPAAm-*g*-PLCL (a) films and (b) nanofibers in deionized water subjected to the alternation of temperature between 25 and 40 °C.

est among all the samples. Meanwhile, PNIPAAm-*g*-PLCL films prepared with 5 kGy irradiation were the least responsive to the temperature change. The deswelling at the elevated temperature is attributed to the loss of hydrophilic interactions among amide groups in PNIPAAm chains.[50] As the hydrophilic interactions are lost, the hydrophobic groups in the PNIAAm network tend to form an aggregated structure. The thermally induced hydrophobic interactions enforce the collapse of the expanded chains formed at the lower temperature, leading to the elimination of internally diffused water. Although the grafted PNIPAAm hydrogels on the PLCL substrates undergo temperature-dependent phase separation, a small amount of water may be trapped within the hydrogels, which may explain the discrepancy between swelling and deswelling ratio of all the samples.

We next investigated the temperature-dependant swelling behavior of PNIPAAm-*g*-PLCL samples by incubation at four different temperatures (25, 30, 37, and 40 °C). PNIPAAm-*g*-PLCL films and nanofibers prepared with 10 kGy irradiation showed significant changes in swelling ratio when the temperature changed from 30 to 37 °C (Figure 6). These results are consistent with the lower critical solution temperature (LCST) characteristics of PNIPAAm; PNIPAAm in water

exhibits a reversible phase transition around 32 °C.[19] The swelling ratio of PNIPAAm-*g*-PLCL films and nanofibers (prepared with 10 kGy) decreased from 2.50 ± 0.67 to 0.85 ± 0.47% and from 37.47 ± 15.88 to 21.21 ± 2.91%, respectively, when the temperature dropped from 37 to 30 °C. However, PNIPAAm-*g*-PLCL films and nanofibers (prepared with 5 kGy) maintained a similar level of swelling ratio irrespective of the temperature change, which may be due to their relatively low graft yields.

Pulsatile swelling processes in samples proved to be repeatable with temperature changes (Figure 7). The PNIPAAm-*g*-PLCL nanofibers (5 and 10 kGy) rapidly responded to temperature change, whereas the swelling ratios of the PLCL films were unchanged during the swelling and deswelling process.

***In vitro* Release Kinetics of IMC and FITC-BSA.** Figures 8(a) and (b) show the release profiles of IMC and FITC-BSA released from PNIPAAm-*g*-PLCL films (10 kGy) and nanofibers (10 kGy) in deionized water in response to the temperature alternating between 25 and 40 °C. We chose two model drugs to prove the efficacy of PNIPAAm-*g*-PLCL substrates for the delivery of hydrophobic as well as hydrophilic molecules. The cumulative amount of IMC and FITC-BSA released from the PNIPAAm-*g*-PLCL substrates was 8.5 ± 2.2 and 13.3 ± 2.3 μg/mL, respectively, after three cycles of repeated temperature changes between 25 and 40 °C. Figure 8(c) shows the pulsatile release rate based on the release profiles. Distinct pulsed drug release kinetics form the PNIPAAm-*g*-PLCL nanofibers were observed; the release rate was significantly higher at 40 °C. The deswelling and the increased molecular motion energy at the elevated temperature may have induced the release of the incorporated drugs from the PNIPAAm-*g*-PLCL substrates. Consistent with previous results, the release rate

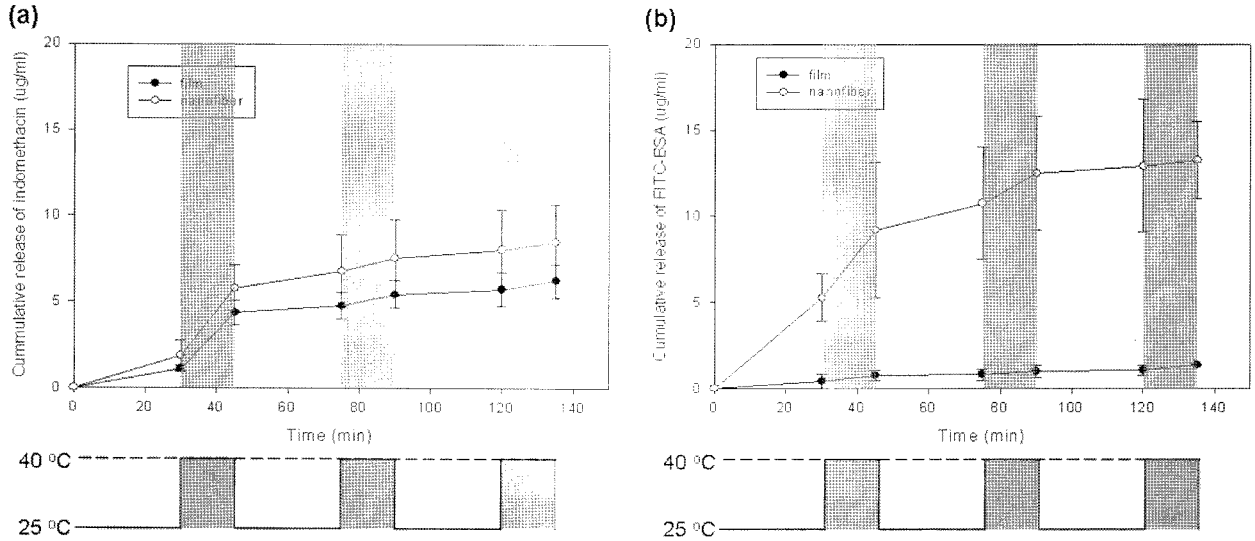

(C)

Model drug	Sample types	Release rate (ug/min)					
Indomethacin	PNIPAAm-g-PLCL film	0.0378 ±0.0147	0.2155 ±0.0531	0.0142 ±0.0065	0.0432 ±0.0051	0.0103 ±0.0023	0.0331 ±0.0079
	PNIPAAm-g-PLCL nanofiber	0.0630 ±0.0102	0.2611 ±0.0432	0.0331 ±0.0153	0.0513 ±0.0074	0.0160 ±0.0045	0.0291 ±0.0065
FITC-BSA	PNIPAAm-g-PLCL film	0.0139 ±0.0014	0.0245 ±0.0023	0.0008 ±0.0001	0.0138 ±0.0026	0.0014 ±0.0003	0.0212 ±0.0014
	PNIPAAm-g-PLCL nanofiber	0.1759 ±0.0423	0.2613 ±0.0663	0.0520 ±0.0025	0.1154 ±0.0521	0.0148 ±0.0039	0.0224 ±0.0095

40 °C
25 °C

Figure 8. Cumulative pulsatile release kinetics of (a) indomethacin and (b) FITC-BSA and (c) release rate of PNIPAAm-*g*-PLCL films and nanofibers in deionized water in response to temperature change between 25 and 40 °C.

from the nanofibers was greater than that from the films.[51] Therefore, the pulsatile release rate and the amount of drug/protein released were controlled by both the deswelling kinetic speed and the grafted PNIPAAm contents of the surface substrates, which were considered to be important parameters for controlled release using temperature-sensitive nanofibers. Although the PNIPAAm-*g*-PLCL nanofibers demonstrated temperature-sensitive release of IMC and FITC-BSA, the ability of the substrate to respond to the external stimuli seems to be reduced by the repeated experiments. The control of the amount of PNIAAm and size of nanofibers can be further optimized to maximize the number of repeatable release of desirable drugs in response to the temperature change.

Conclusions

In this study, we prepared PNIPAAm-*g*-PLCL films and nanofibers using gamma-ray irradiation. The graft yield increased with an increase in the irradiation dose. In addition, under the same irradiation condition PLCL nanofibers allowed for greater graft yield compared to PLCL films due to their higher surface area to volume ratio. All the samples grafted with PNIAAm reached an equilibrium swelling/deswelling stage within 10 min. The equilibrium swelling ratio increased with the increase in the irradiation dose. The swelling ratio of samples showed temperature-dependent collapse from the swollen state when the samples were placed from 30 to 37 °C; the temperature-sensitive swelling change was reversible. The swelling ratio of PNIPAAm-g-PLCL nanofibers prepared by irradiation of 10 kGy was the greatest among the samples. It was also found that the release of model drugs, IMC and FITC-BSA could be controlled by the pulsed temperature change. Collectively, temperature-sensitive PNIPAAm-*g*-PLCL electrospun nanofibers, due to their simple fabrication method combined with the surface grafting technique and effective controlled swelling behavior in response to physiological temperature changes, can be used for drug delivery carriers for various biomedical applications.

Acknowledgements. This research was supported by a grant from the Nuclear Research and Development Program funded by the Ministry of Science and Technology, Korea. S.I.J. is very grateful to the BK21 Project for a fellowship.

References

(1) K. Jayaraman, M. Kotaki, Y. Z. Zhang, X. M. Mo, and S. Ramakrishna, *J. Nanosci. Nanotechno.*, **4**, 52 (2004).
(2) D. H. Reneker, A. L. Yarin, E. Zussman, and H. Xu, *Adv. Appl. Mech.*, **41**, 43 (2007).
(3) T. Courtney, M. S. Sacks, J. Stankus, J. Guan, and W. R. Wagner, *Biomaterials*, **27**, 3631 (2006).
(4) L. S. Nair, S. Bhattacharyya, and C. T. Laurencin, *Expert Opin. Biol. Th.*, **4**, 659 (2004).
(5) M. Goldberg, R. Langer, and X. Q. Jia, *J. Biomat. Sci. Polym. E.*, **18**, 241 (2007).
(6) Z. Jing, X. Y. Xu, X. S. Chen, Q. Z. Liang, X. C. Bian, L. X. Yang, and X. B. Jing, *J. Control. Release*, **92**, 227 (2003).
(7) K. Kim, Y. K. Luu, C. Chang, D. F. Fang, B. S. Hsiao, B. Chu, and M. Hadjiargyrou, *J. Control. Release*, **98**, 47 (2004).
(8) Z. W. Ma, M. Kotaki, R. Inai, and S. Ramakrishna, *Tissue Eng.*, **11**, 101 (2005).
(9) J. Venugopal and S. Ramakrishna, *Appl. Biochem. Biotech.*, **125**, 147 (2005).
(10) Y. Z. Zhang, X. Wang, Y. Feng, J. Li, C. T. Lim, and S. Ramakrishna, *Biomacromolecules*, **7**, 1049 (2006).
(11) T. Takezawa, *Biomaterials*, **24**, 2267 (2003).
(12) E. K. Jeon, H. J. Whang, G. Khang, I. Lee, J. M. Rhee, and H. B. Lee, *Polymer(Korea)*, **25**, 893 (2001).
(13) H. C. Kroese-Deutman, P. Q. Ruhe, P. H. M. Spauwen, and J. A. Jansen, *Biomaterials*, **26**, 1131 (2005).
(14) J. Sohier, R. E. Haan, K. de Groot, and J. M. Bezemer, *J. Control. Release*, **87**, 57 (2003).
(15) P. K. D. V. Yarlagadda, M. Chandrasekharan, and J. Y. M. Shyan, *Bio-Med. Mater. Eng.*, **15**, 159 (2005).
(16) Y. F. Zhang, X. R. Cheng, J. W. Wang, Y. N. Wang, B. Shi, C. Huang, X. C. Yang, and T. J. Liu, *Biochem. Bioph. Res. Co.*, **344**, 362 (2006).
(17) X. D. Xu, H. Wei, X. Z. Zhang, S. X. Cheng, and R. X. Zhuo, *J. Biomed. Mater. Res. A*, **81A**, 418 (2007).
(18) X. Z. Zhang, P. J. Lewis, and C. C. Chu, *Biomaterials*, **26**, 3299 (2005).
(19) H. K. Ju, S. Y. Kim, and Y. M. Lee, *Polymer*, **42**, 6851 (2001).
(20) J. H. Kim, S. B. Lee, S. J. Kim, and Y. M. Lee, *Polymer*, **43**, 7549 (2002).
(21) S. Y. Kim, S. M. Cho, Y. M. Lee, and S. J. Kim, *J. Appl. Polym. Sci.*, **78**, 1381 (2000).
(22) M. K. Yoo, Y. K. Sung, Y. M. Lee, and C. S. Cho, *Polymer*, **41**, 5713 (2000).
(23) M. L. Zhai, N. Liu, J. Li, M. Yi, J. Q. Li, and H. F. Ha, *Radiat. Phys. Chem.*, **57**, 481 (2000).
(24) H. Zhang, L. Y. Chu, Y. K. Li, and Y. M. Lee, *Polymer*, **48**, 1718 (2007).
(25) E. H. Cho, S. G. Lee, and J. K. Kim, *Curr. Appl. Phys.*, **5**, 475 (2005).
(26) J. K. Shim, H. S. Na, Y. M. Lee, H. Huh, and Y. C. Nho, *J. Membrane Sci.*, **190**, 215 (2001).
(27) Y. Yang, M. C. Porte, P. Marmey, A. J. El Haj, J. Amedee, and C. Baquey, *Nucl. Instrum. Meth. B*, **207**, 165 (2003).
(28) C. H. Zhang, Y. D. Huang, and Y. D. Zhao, *Mater. Chem. Phys.*, **92**, 245 (2005).
(29) H. Haugen, L. C. Gerhardt, J. Will, and E. Wintermantel, *J. Biomed. Mater. Res. B*, **73B**, 229 (2005).
(30) H. J. Haugen, M. Brunner, F. Pellikofer, J. Aigner, J. Will, and E. Wintermantel, *J. Biomed. Mater. Res. B*, **80B**, 415 (2007).
(31) F. H. Lin, T. M. Chen, K. S. Chen, T. H. Wu, and C. C. Chen, *Mater. Chem. Phys.*, **64**, 189 (2000).
(32) R. E. Shariatpanahi, F. Orang, S. H. Emami, and T. Naimi, *J. Biomat. Sci. Polym. E.*, **17**, 659 (2006).
(33) R. L. Dunn, G. L. Yewey, S. M. Fujita, K. R. Josephs, S. L.

Whitman, G. L. Southard, W. S. Dernell, R. C. Straw, S. J. Withrow, and B. E. Powers, *J. Bioact. Compat. Pol.*, **11**, 286 (1996).
(34) S. I. Jeong, J. H. Kwon, J. I. Lim, S. W. Cho, Y. M. Jung, W. J. Sung, S. H. Kim, Y. H. Kim, Y. M. Lee, B. S. Kim, C. Y. Choi, and S. J. Kim, *Biomaterials*, **26**, 1405 (2005).
(35) Y. B. Zhu, M. F. Leong, W. F. Ong, M. B. Chan-Park, and K. S. Chian, *Biomaterials*, **28**, 861 (2007).
(36) S. I. Jeong, B. S. Kim, Y. M. Lee, K. J. Ihn, S. H. Kim, and Y. H. Kim, *Biomacromolecules*, **5**, 1303 (2004).
(37) S. I. Jeong, S. H. Kim, Y. H. Kim, Y. Jung, J. H. Kwon, B. S. Kim, and Y. M. Lee, *J. Biomat. Sci. Polym. E.*, **15**, 645 (2004).
(38) E. Arenas, E. Bucio, G. Burillo, and G. P. Lopez, *Polym. Bull.*, **58**, 401 (2007).
(39) S. B. Lee, E. K. Park, Y. M. Lim, S. K. Cho, S. Y. Kim, Y. M. Lee, and Y. C. Nho, *J. Appl. Polym. Sci.*, **100**, 4439 (2006).
(40) Q. Liu, Z. Y. Zhu, X. M. Yang, X. L. Chen, and Y. F. Song, *Radiat. Phys. Chem.*, **76**, 707 (2007).
(41) S. B. Lee, S. M. Seo, Y. M. Lim, S. K. Cho, Y. M. Lee, and Y. C. Nho, *Macromol. Res.*, **12**, 269 (2004).
(42) L. Grondahl, F. Cardona, K. Chiem, and E. Wentrup-Byrne, *J. Appl. Polym. Sci.*, **86**, 2550 (2002).
(43) S. Kimura, K. Yasuda, N. Hara, T. Sakai, S. Mikami, A. Minami, and H. Tohyama, *Arthroscopy*, **19**, 68 (2003).
(44) K. Kesenci, A. Motta, L. Fambri, and C. Migliaresi, *J. Biomat. Sci. Polym. E.*, **12**, 337 (2001).
(45) S. Q. Liu, Y. Y. Yang, X. M. Liu, and Y. W. Tong, *Biomacromolecules*, **4**, 1784 (2003).
(46) E. Bucio, E. Arenas, and G. Burillo, *Mol. Cryst. Liq. Cryst.*, **447**, 521 (2006).
(47) T. Peng and Y. L. Cheng, *J. Appl. Polym. Sci.*, **70**, 2133 (1998).
(48) Y. Kaneko, R. Yoshida, K. Sakai, Y. Sakurai, and T. Okano, *J. Membrane Sci.*, **101**, 13 (1995).
(49) R. Yoshida, K. Uchida, Y. Kaneko, K. Sakai, A. Kikuchi, Y. Sakurai, and T. Okano, *Nature*, **374**, 240 (1995).
(50) J.-h. Kim and T. R. Lee, *Langmuir*, **23**, 6506 (2007).
(51) W. Cui, X. Li, X. Zhu, G. Yu, S. Zhou, and J. Weng, *Biomacromolecules*, **7**, 1623 (2006).